



# Esterification of levulinic acid via catalytic and photocatalytic processes using fluorinated titanium dioxide materials

Esterificación de ácido levulínico mediante procesos catalíticos y fotocatalíticos empleando dióxido de titanio fluorado

Claudia Castañeda <sup>1</sup>, José J. Martínez <sup>1</sup>, Andrés Mesa<sup>1</sup>

<sup>1</sup>Grupo de Catálisis-UPTC, Escuela de Ciencias Química, Universidad Pedagógica y Tecnológica de Colombia. Sede Central Tunja, Boyacá, Colombia Avenida Central del Norte 39-115. A. A. 1094. Boyacá, Colombia

## CITE THIS ARTICLE AS:

C. Castañeda, J. J. Martínez and A. Mesa. "Esterification of levulinic acid via catalytic and photocatalytic processes using fluorinated titanium dioxide materials", *Revista Facultad de Ingeniería Universidad de Antioquia*, no. 105, pp. 29-36, Oct-Dec 2022. [Online]. Available: <https://www.doi.org/10.17533/udea.redin.20210531>

## ARTICLE INFO:

Received: August 21, 2020

Accepted: May 17, 2021

Available online: May 24, 2021

## KEYWORDS:

Catalysis; photocatalysis; levulinic acid; esterification;  $TiO_2 - F$

Catálisis; fotocatalisis; ácido levulínico; esterificación;  $TiO_2 - F$

**ABSTRACT:** This study evaluated the synthesis, characterization, and activity of fluorinated titanium dioxide materials ( $TiO_2 - F1\%$  and  $TiO_2 - F5\%$ ) *in-situ* modified by the sol-gel method in the esterification reaction of levulinic acid conducted by catalytic and photocatalytic processes. The physicochemical properties of the materials were determined by X-ray diffraction, UV-Vis diffuse reflectance spectroscopy, thermal analysis, and pyridine adsorption. It was found that the inclusion of fluoride anion causes a decrease in the levulinic acid conversion by photocatalytic reaction; however, in the catalytic activation, a slight increase in the conversion using the fluoride materials was observed. Finally, the reaction in the presence of halogenated solvents ( $CCl_4$ ) by photolysis reaction favors a conversion of 100% in 1h.

**RESUMEN:** En el presente trabajo de investigación se estudió la síntesis, caracterización y actividad de materiales de dióxido de titanio fluorados ( $TiO_2 - F1\%$  y  $TiO_2 - F5\%$ ) modificados *in-situ* a través del método de sol-gel, en la reacción de esterificación de ácido levulínico conducida tanto por vía fotocatalítica como catalítica. Las propiedades fisicoquímicas de los materiales se determinaron mediante estudios por difracción de rayos X, espectrofotometría UV-Vis de reflectancia difusa, análisis térmico y adsorción de piridina. Se encontró que la inclusión del anión fluoruro causa una disminución en la conversión del ácido levulínico por vía fotocatalítica; sin embargo, en la activación por vía catalítica se observó un ligero incremento en la conversión del ácido levulínico empleando los materiales fluorados. Finalmente, la reacción en presencia de disolventes halogenados ( $CCl_4$ ) mediante reacción de fotólisis favorece una conversión del 100% en 1h.

## 1. Introduction

In recent years, the conversion of biomass and its respective derivatives has represented a topic of great interest due to the possibility of being considered as an alternative source for the sustainable production of biofuels and raw materials [1, 2]. The platform compounds obtained from biomass include the levulinic acid (LA), which is considered a raw material for the synthesis of

various organic compounds such as levulinate esters,  $\gamma$ -valerolactone, acrylic acid,  $\beta$ -acetylacrylic acid, and  $\delta$ -aminolevulinic acid, among others [3]. In particular, levulinate esters have important applications in industrial processes as plasticizing agents, solvents, and fragrances [4, 5]; in addition, they can be used as additives in fuels [6] due to their lubricating properties and stability of the flash point [7]. A particular case is the ethyl levulinate, which is recognized for its use as an additive in gasoline and biodiesel [7]. Additionally, the esters derived from levulinic acid are raw materials for the conversion of high added value compounds, such as:  $\gamma$ -valerolactone [8].

In general, the esterification reactions of levulinic acid are

\* Corresponding author: Claudia Castañeda

E-mail: [claudia.castaneda.mar@gmail.com](mailto:claudia.castaneda.mar@gmail.com)

ISSN 0120-6230

e-ISSN 2422-2844

carried out in the presence of an acid catalyst, such as sulfuric, polyphosphoric, or nitric acid, in a homogeneous medium [4]. In the case of the synthesis of butyl levulinate (Scheme 1), an intermediate known as pseudo butyl levulinate is formed, both products are very significant, and the selectivity can be oriented by the use of weak acidic solids.

However, the use of conventional liquid acids generates environmental problems associated with the handling, disposal, and regeneration due to their corrosive and toxic nature. A possible solution is the use of acid solids; however, some of these could cause leaching, for example, the heteropolyacids [9]; besides, the reaction requires high reaction temperatures, which is due to the displacement of the equilibrium by the water formed. In this sense, it is necessary to find solids that simultaneously conduct the reaction without leaching of the active phase and to explore green methodologies that allow reducing reaction temperatures. Therefore, photocatalysis can be a novel alternative to revert this problem [10].

Nevertheless, few studies have been reported for esterification assisted by photocatalysis; some of these are, for example, the study developed by Verma *et al.* [11], who studied the reactions of esterification of acetic acid with methanol by photocatalytic induction using solids of  $SO_4/TiO_2$  and impregnated with  $H_2SO_4$  and  $HCl$ . The authors reported a conversion of 79% compared to commercial  $TiO_2$ , where it is only 35%. In order to clarify the effect of the acid, a reaction was carried out using  $H_2SO_4$  as a catalyst, and only 10% conversion was obtained. The authors concluded that the activation of the  $TiO_2$  catalysts with  $H_2SO_4$  allowed the formation of  $O - Ti - SO_3H$  sites (acid complex) that favored the esterification reactions and proposed a mechanism through the formation of free radicals.

On the other hand, Cardoso *et al.* [12] optimized the reaction conditions in the esterification of oleic acid using methanol, achieving conversions of 59% employing  $TiO_2$  nanotubes and 85% with commercial  $TiO_2$ . The researchers concluded that the use of strong stirring favors the esterification process and that photocatalysts with highly hydroxylated surfaces could affect the conversion to the esters. Corro *et al.* [13] used  $ZnO/SiO_2$  solids in the production of biodiesel under photocatalytic conditions. The authors reported that with the use of this type of materials, a conversion close to 93% was achieved, while when the reaction is conducted in the absence of radiation, the conversion was only 2%. Activation of the solids by UV radiation favored the reaction in the esterification stage, and this itself in a basic medium induced the formation of biodiesel. Thus, it can be indicated that there are no studies related to

the esterification of levulinic acid under photocatalytic conditions; for that reason, the panorama of this reaction under these conditions is a new field of research.

On the other hand, one of the semiconductors frequently used in photocatalysis is  $TiO_2$ , whose performance is strongly dependent on its optical, electronic, morphological, crystalline, and surface chemistry properties [14, 15], which can be optimized by modifying the semiconductor with metallic and non-metallic elements. Modification of  $TiO_2$  with anions has been preferred over the use of cations since anions tend to form fewer recombination centers on the surface of titanium dioxide [16].

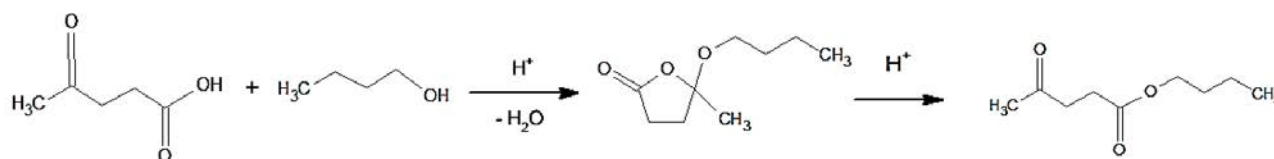
The replacement of an oxygen or titanium site with a differently charged element can introduce a charge imbalance, which results in the formation of specific crystallographic defects such as oxygen or titanium vacancies. However, in doped  $TiO_2$ , the associated charge imbalance is compensated by the oxidation state change of the dopant or any atom of  $TiO_2$ . For example, the substitution of oxygen by fluoride ions ( $F^-$  would occupy an  $O^{2-}$  site) considers a change of oxidation state from  $Ti^{4+}$  to  $Ti^{3+}$  [17]. In photocatalytic processes,  $Ti^{3+}$  surface states could trap photogenerated electrons and then transfer them to species adsorbed on the  $TiO_2$  surface [18]. On the other hand, if the modification of titanium dioxide with fluorine occurs at the surface level, these species can trap the electrons in the conduction band with higher intensity due to the high electronegativity of fluorine and then transfer them to the adsorbed species in the semiconductor surface, thereby reducing the recombination frequency of the photogenerated electron-hole pairs [19].

In this study, the synthesis and characterization of *in-situ* modified  $TiO_2$  materials are proposed through a fluorination process, and the evaluation of their activity in the levulinic acid esterification reaction conducted both catalytically and photocatalytically.

## 2. Experimental section

### 2.1 Synthesis of the catalysts

The reference  $TiO_2$  photocatalyst was synthesized by the conventional sol-gel route. The titanium butoxide precursors, butyl alcohol, and the hydrolysis catalyst, nitric acid (0.5mL), were added to a glass flask, and the mixture was homogenized at 40°C with constant stirring for 2 h. In order to start the hydrolysis and condensation processes, distilled water in ethyl alcohol was added, and the solution was added dropwise to the initial precursor



**Scheme 1** Synthesis of pseudo butyl levulinate and butyl levulinate

mixture. The molar ratio of titanium butoxide: water: butyl alcohol used in the synthesis was 1:8:35, respectively. Subsequently, the system was maintained at reflux for 24 h at 75°C under vigorous stirring. Then, the gel obtained was dried at 85°C for 48 h in order to eliminate solvent residues. The dry material was grounded in an agate mortar. Finally, the solid was calcinated at 400°C for 6 h using a heating ramp of 0.5C/min.

Fluorinated titanium dioxide photocatalysts ( $TiO_2 - F$ ) were synthesized by *in-situ* fluorination of  $TiO_2$  using the sol-gel method, following the steps described for the reference material. In this case, ammonium fluoride was used as a hydrolysis catalyst and as an anionic precursor. In order to evaluate the effect of the anion content in the material, the photocatalysts with different percentages of fluoride were synthesized, specifically at 1.0wt% and 5.0wt%. The materials were labeled  $TiO_2F$  1% and  $TiO_2F$  5%.

## 2.2 Characterization of the catalysts

The identification of the crystalline phases present in the materials was carried out by X-ray diffraction studies, developed on a Bruker D2 Phaser diffractometer using a  $CuK\alpha$  radiation ( $\lambda = 0.15405$  nm). The analysis was performed in the range of 20 from 10 to 80 with a step of 0.02 and a count time of 0.6s.

UV-Vis diffuse reflectance spectra were obtained on a Cary 100 UV-Vis spectrophotometer, equipped with an integrating sphere. The prohibited band energy values were calculated considering the indirect transitions of the  $TiO_2$  semiconductor, by linear adjustment of the slope to the abscissa of the modified Kubelka - Munk equation  $[F(R) \times hv]^{1/2}$  as a function of absorbed light energy.

Thermogravimetric analyzes were performed on an Infinity PRO thermal analyzer at a temperature range between 25°C and 700°C, using a heating ramp of 10°C/min, and supplying an air flow of 5 mL/min.

Pyridine adsorption analyzes were obtained *in-situ* using an Infrared Fourier Transform Spectrometer Nicolet IS50 equipped with a diffuse reflectance cell. The solids were pretreated by heating to 350°C using a Helium flow at 30 mL/min for 2 h. Then the sample was cooled to

30°C to begin the pyridine adsorption using a Helium flow at 15 mL/min; the saturation times ranged from 20 to 40 min. The pyridine was desorbed by raising the temperature from 50°C to 350°C.

## 2.3 Evaluation of the catalytic activity

Levulinic acid esterification was studied in a glass reactor, adding levulinic acid/n-butanol in a molar ratio (1:4). After the homogenization of the reactants, 10% of the catalytic material with respect to the mass of the levulinic acid was added to the reactor. The reaction system was maintained at 60°C with constant stirring at 500rpm for 5 h, and aliquots were extracted every hour.

Photocatalytic levulinic acid esterification was carried out following the procedure described above, but the levulinic acid was allowed to adsorb on the solid for 10 minutes with constant stirring at 500rpm in the absence of radiation. Subsequently, the system was irradiated with a Pen Ray Power Supply lamp (UV lamp, emitting at 254 nm, 4.4 mW), protected by a quartz tube. The reaction was maintained under constant stirring for 5 h.

The esterification reactions were monitored using a Varian 3800 gas chromatograph, using a 30 m  $\times$  0.25 mm  $\times$  0.25  $\mu$ m RTX- 5 column and Helium as stripping gas.

## 3. Results and discussion

### 3.1 Characterization of the catalysts

The diffraction patterns of the materials  $TiO_2$ ,  $TiO_2 - F$  1 %, and  $TiO_2 - F$  5 % are presented in Figure 1. As can be seen, the three solids present the characteristic signals of the anatase polymorph of titanium dioxide at 25°(101), 37.8°(004), 48.1°(200), 53.9°(105), 55.1°(211), 62.6°(204). Signals associated with the rutile phase were not evidenced, suggesting that *in-situ* fluorination stabilizes the crystalline structure of the semiconductor. A detailed observation of the diffraction signals shows that an increase in the fluoride content generates an increase in crystallinity and the formation of larger crystallites compared with the reference material; these

characteristics are manifested in the formation of more intense diffraction signals and with a narrow medium width.

The average size of the crystallite was estimated from the magnification of the signal to  $25^\circ$  corresponding to the plane  $(1\ 0\ 1)$  and using the Scherrer equation (Table 1). The calculated crystallite size for the  $TiO_2$  catalyst is 10.1 nm. However, when the semiconductor is modified with 5% of fluoride, sizes close to 13.9 nm are obtained. These results confirm that the presence of fluoride ions promotes the crystallization and the growth of anatase crystallites; similar results were previously reported [18–20].

**Table 1** Crystallite size and energy gap of the studied solids

Catalyst	Crystallite Size (nm)	$E_g(eV)$
$TiO_2$	10.1	3.01
$TiO_2 - F\ 1\ \%$	12.6	2.98
$TiO_2 - F\ 5\ \%$	13.9	2.98

The optical response of the  $TiO_2$  and the modified solids were studied by UV-Vis Diffuse reflectance spectrometry in the range between 300 – 500 nm (Figure 2a)). Around 411 nm, the typical absorption edge of  $TiO_2$  can be observed. Regarding the modified materials, strong absorption in the ultraviolet region and a slight displacement towards higher wavelengths were evidenced. The energy gap ( $E_g$ ) values were calculated from the modified Kubelka-Munk plot in the function of the absorbed light energy (Figure 2b)) and these are presented in Table 1. The  $E_g$ , calculated for the reference  $TiO_2$  and the fluorinated materials differ by 0.03eV, indicating that *in-situ* fluorination of the semiconductor does not cause a significant modification in its electronic properties.

The thermal behavior of the materials was studied by thermal analysis, and the results are presented in Figure 3. As can be seen in the thermograms, the estimated total mass loss for the  $TiO_2$ ,  $TiO_2F\ 1\%$ , and  $TiO_2F\ 5\%$  solids were 12.1%, 21.9%, and 21.8%, respectively. In the case of  $TiO_2$  (Figure 3a)), in a first stage in the range of  $25^\circ C$  to  $125^\circ C$ , there was a loss of mass of approximately 4.6% due to the evaporation of water and organic solvent remaining from the synthesis [18]. In a second stage, including the range of  $125^\circ C$  to  $230^\circ C$ , a loss of mass of 2.7% was observed, which is associated with the elimination of chemisorbed hydroxyl groups [21]. Finally, in the segment from  $230^\circ C$  to  $420^\circ C$ , a loss of mass of around 4.7% was observed, which is associated with oxidation residues from carbon and chemisorbed water in the solids [22]. Regarding the solids modified,  $TiO_2F\ 1\%$  and  $TiO_2F\ 5\%$ , in the second phase, the mass losses of the solids were 8.2% and 7.7%, respectively; and in the third phase of 7.6% and 6.6%, respectively, as is seen in Figures

3b) and 3c). The reduction of the masses during the heat treatment is higher in the solids modified with respect to the reference  $TiO_2$ . Possibly, this result is a consequence of the degree of hydroxylation of the solids generated during the gelation process of titanium n-butoxide in the presence of fluoride ions.

On the other hand, the DSC curves show three main signals both in the  $TiO_2$  solid and in the modified samples. In the range of  $50^\circ C$  to  $100^\circ C$ , a weak endothermic signal associated with the desorption of water is observed. The  $TiO_2$  solid shows an exothermic signal at  $273^\circ C$ ; in the modified solids, it is observed at  $255^\circ C$ , corresponding to the dehydration and decomposition of the organic substances contained in the xerogel. Finally, around  $400^\circ C$ , an exothermic signal related to the combustion of residual organic compounds is evidenced [21].

The infrared spectra of pyridine adsorbed from the samples are presented in Figure 4. As can be seen, the three solids presented signals located between  $1445\text{cm}^{-1}$  and  $1605\text{cm}^{-1}$ , which have been related to Lewis acid sites [23, 24]. In this sense, the modification with fluoride ions does not modify the type of acidity of  $TiO_2$ .

### 3.2 Evaluation of the catalytic activity

The materials were evaluated in the esterification reactions of levulinic acid with butanol; the acid:alcohol ratio and percentage of the catalyst used is the same as that reported by other authors [11, 12, 25]. The esterification process in the absence of catalytic material (Blank) shows that levulinic acid can act as an autocatalyst for the reaction. Table 2 summarizes the specific activity and selectivity towards the esters obtained without photocatalytic activation at an isoconversion of 10%.

The order of catalytic activity was  $TiO_2 - F5\% \approx TiO_2 - F1\% > TiO_2 > \text{Blank}$ . Consequently, at the same conversion (10%), it can be seen that the presence of fluoride ions can improve the conversion of  $TiO_2$ . Regarding selectivity, pseudo butyl levulinate (pBL) and butyl levulinate (BL) are obtained. Al-Shaal *et al.* [26] described that the activation energy for the formation of pseudo butyl levulinate and butyl levulinate is 3 and 50 kJ/mol, respectively. Therefore, Lewis acid sites, such as those found in the modified solids, are sufficient to allow the formation of pBL and BL. However, the high barrier of the *trans*-esterification of pBL to BL is considerably higher, and therefore, the catalyst is not capable of transforming all pBL to BL, which is best evident at low conversions (Table 2).

The reactions via photocatalytic activation were carried out using a lamp with a wavelength of 254 nm (considering the

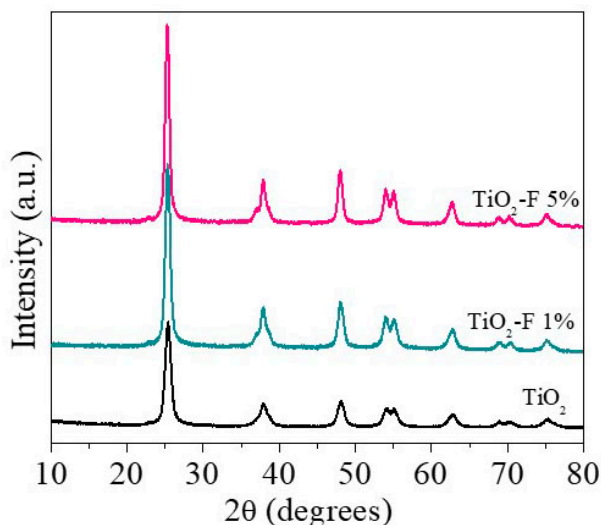


Figure 1 XRD patterns for  $TiO_2$  and  $TiO_2 - F$  samples

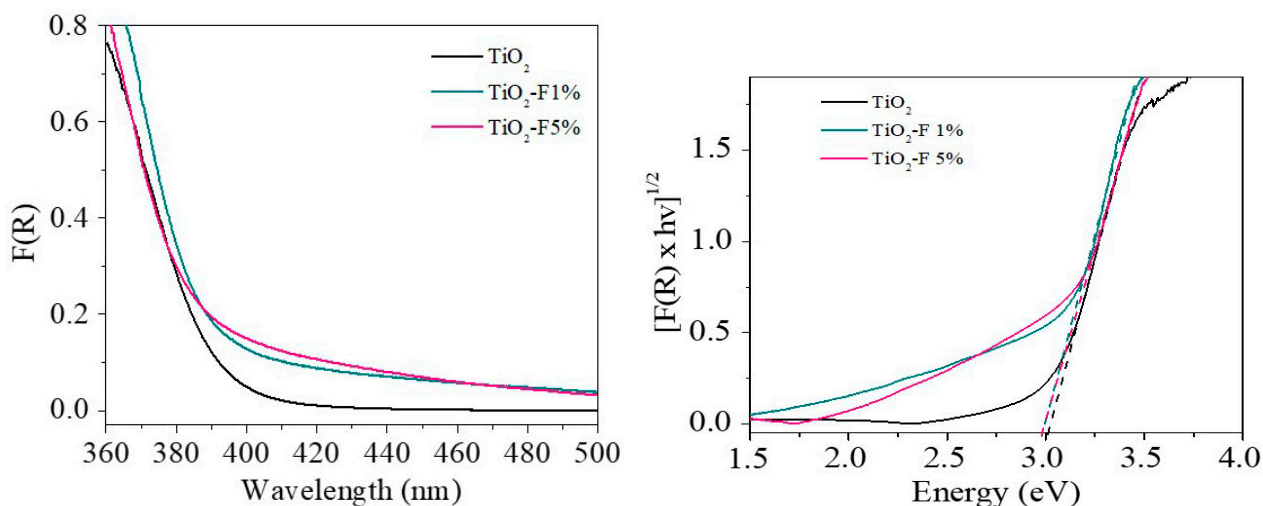


Figure 2 a) UV-Vis DRS of  $TiO_2$  and  $TiO_2 - F$  samples. b) Kubelka-Munk modified spectra for studied samples

Table 2 Results of the esterification of levulinic acid with butanol at an iso-conversion of 10%

Catalyst	Specific Rate ( $mol/hg^*$ )	Sel. pBL(%)	Sel. BL (%)
Blank	1.22	85	15
$TiO_2$	2.43	84	16
$TiO_2 - F1\%$	4.80	90	10
$TiO_2 - F5\%$	4.84	90	10

results obtained from  $E_g$ ); the temperature reached was  $60^\circ C$ , which allows the results can be compared with the reactions conducted by the catalytic route. In Table 3, at an iso-conversion of 10%, it can be seen that the order of activity is  $Blank \approx TiO_2 > TiO_2 - F1\% > TiO_2 - F5\%$ . Contrary to catalytically driven reactions, fluoride ions do not improve photocatalytic activity. The esters obtained are the same as in the catalytic esterification reactions; however, by photocatalysis, the presence of other compounds from the photolysis of butanol was observed

(Table 3): Thus, butanal and others are formed as majority products [24]. This photolytic reaction is believed to affect the reaction via the photocatalytic route, possibly by poisoning the catalysts and consequently decreasing the conversion of levulinic acid.

To corroborate the effect of photolysis and considering that the presence of halogenated solvents produces highly reactive free radicals that can react with alcohol to form  $HCl$  *in-situ* and favor the esterification reaction

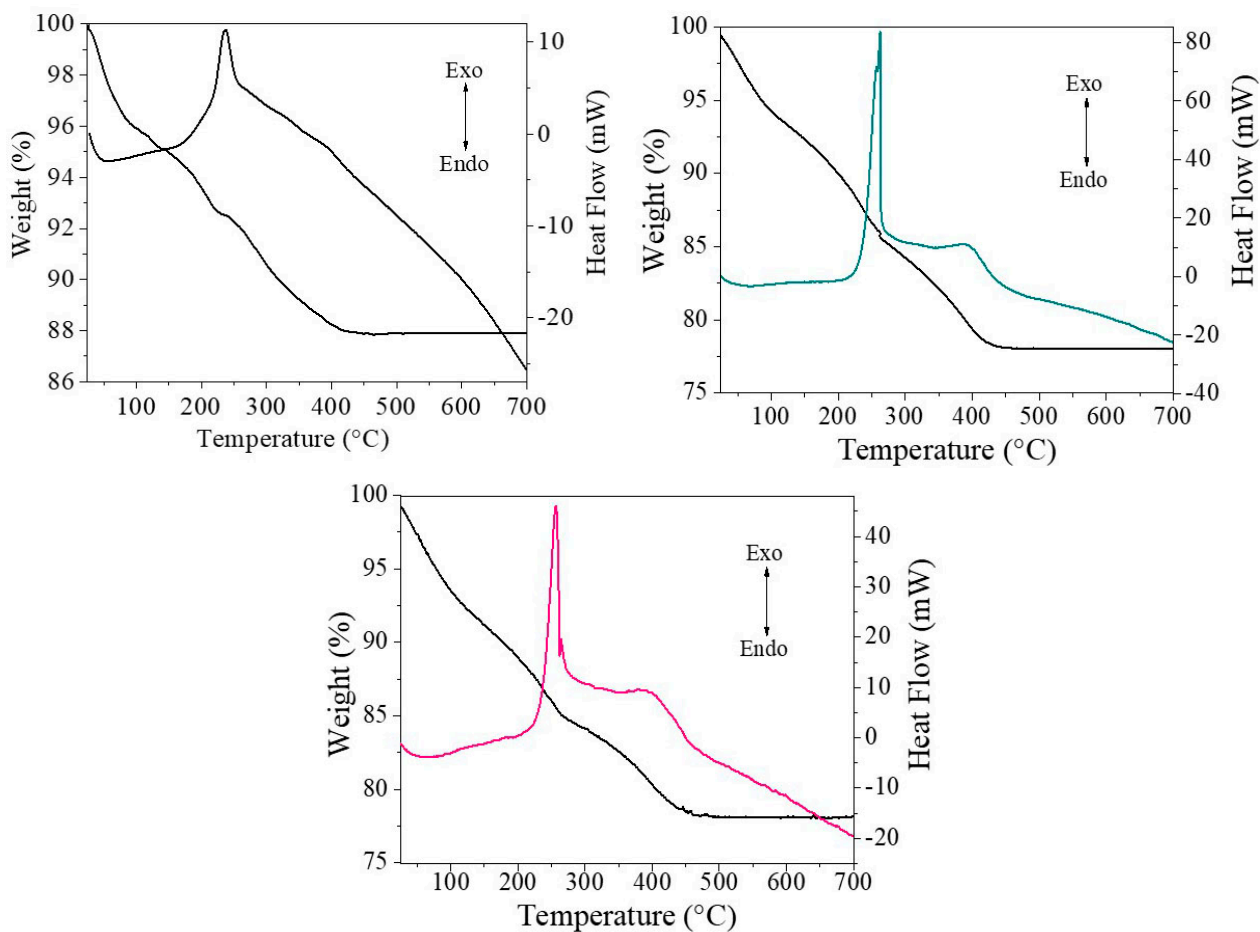


**Figure 3** DSC and TGA curves of a)  $TiO_2$ , b)  $TiO_2F1\%$ , and c)  $TiO_2F5\%$

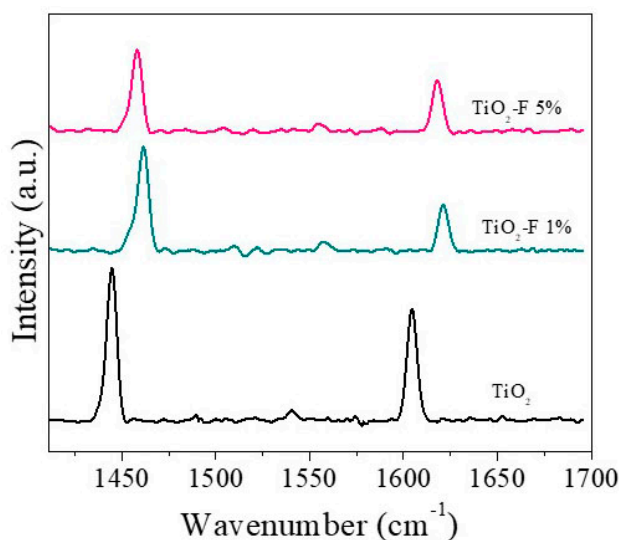


**Figure 4** Diffuse reflectance infrared spectra of adsorbed pyridine of the  $TiO_2$  and  $TiO_2 - F$  materials

[27], photocatalytic esterification with reference  $TiO_2$  and  $TiO_2 - F1\%$  solid were studied in the presence of a chlorinated solvent. The blank reaction results with

an excess of the  $CCl_4$  [4 mL] and, in the absence of catalysts, shows 100% conversions at 1 h of reaction. When the reference  $TiO_2$  is present in the reaction, the

**Table 3** Results of the photocatalytic activity of the esterification of levulinic acid with butanol at an iso-conversion of 10%

Catalyst	Specific Rate ( mol/ h* g)	Sel. p. BL (%)	Sel. BL (%)	Sel. Butanal (%)	Sel. others (%)
Blank	0.91	8	10	43	40
TiO <sub>2</sub>	0.91	14	17	53	15
TiO <sub>2</sub> – F1%	0.49	11	26	69	31
TiO <sub>2</sub> -F 5%	0.41	10	18	50	23
Photolysis of Butanol	1.70	0	0	30	70

**Table 4** Results of the photolytic reaction of the esterification of levulinic acid with butanol in CCl<sub>4</sub> at an iso-conversion of 100%

Catalyst	Sel. pBL (%)	Sel. BL (%)	Sel. Butanal (%)	Sel. Others (%)
Blank	–	79	10	11
TiO <sub>2</sub>	–	82	13	5
TiO <sub>2</sub> – F1%	–	81	13	4
Reuse 1 TiO <sub>2</sub>	–	82	15	3
Reuse 2 TiO <sub>2</sub>	–	81	13	4
Reuse 3 TiO	–	81	12	5

100% conversion is also achieved after 1 h of reaction, but the CCl<sub>4</sub> amount used is four times less (1 mL). Similar results were observed conducting the reaction in the presence of the TiO<sub>2</sub> – F1% solid. These results show that the presence of fluoride does not affect BL performance.

Table 4 summarizes the selectivity obtained at 1 h of reaction (100% conversion). It is interesting to note that pseudo butyl levulinate is not formed, which proves that the esterification conducted in Lewis acid sites leads to the mixing of the pBL and BL esters, but via photolysis, the formation of a Brønsted acid favors the formation of BL. The radical species of alcohol and the acidic medium, which is formed *in situ*, induce the dehydration of carboxylic acid to promote the esterification reaction [27]. The formation of HCl was verified by determining the pH using indicator paper, being close to 2 after the reaction.

The presence of TiO<sub>2</sub> favored the decrease of the other photolysis products, which can be explained considering that the solid acts as a collector of the free radicals of the other species, favoring only the most stable ones and consequently allowing the reaction to be oriented towards a higher obtaining of butyl levulinate. Reuse tests were developed using the reference TiO<sub>2</sub>, and the results obtained demonstrate that the activity of the solid is not affected, which suggests the stability of the material.

## 4. Conclusions

Modification of the TiO<sub>2</sub> materials with fluoride ions did not significantly favor the conversion of levulinic acid by the photocatalytic route using butanol. Additionally, it was found that secondary reactions usually occur by this method severely affecting the solids, such as the photolysis of alcohol that affected the performance of the

catalysts. However, it was found that photolytic reactions with halogenated solvents favor the conversion of levulinic acid, exhibiting conversions of up to 100% and selectivity of 82%.

## 5. Declaration of competing interest

I declare that I have no significant competing interests including financial or non-financial, professional, or personal interests interfering with the full and objective presentation of the work described in this manuscript.

## 6. Acknowledgments

The authors are grateful for the support of Vicerrectoría de Investigación y Extensión, Universidad Pedagógica y Tecnológica de Colombia.

## 7. Funding

This work was supported by Vicerrectoría de Investigación y Extensión, Universidad Pedagógica y Tecnológica de Colombia by the project SGI 3344.

## 8. Author contributions

José Jobanny Martínez: Conceptualization, Formal Analysis, Writing, Supervision. Andres Camilo Mesa: Conceptualization, Formal Analysis, Writing. Claudia Patricia Castañeda: Conceptualization, Formal Analysis, Writing.

## 9. Data availability statement

The authors confirm that the data supporting the findings of this study are available within the article.

## References

- [1] X. Li and *et al.*, "Simultaneous catalytic esterification of carboxylic acids and acetalisation of aldehydes in a fast pyrolysis bio-oil from mallee biomass," *Fuel*, vol. 90, Jul., 2011.
- [2] A. Rodríguez, M. Brijado, L. Rache, L. Silva, and L. Esteves, "Reacciones comunes de Furfural en procesos escalables de Biomasa Residual," *Ciencia en Desarrollo*, vol. 11, Jan., 2020.
- [3] I. Thapa and *et al.*, "Efficient green catalysis for the conversion of fructose to levulinic acid," *Applied Catalysis A: General*, vol. 539, Jun. 5, 2017.
- [4] H. Bart, J. Reidetschlager, K. Schatka, and A. Lehmann, "Kinetics of esterification of levulinic acid with n-butanol by homogeneous catalysis," *Ind. Eng. Chem. Res.*, vol. 33, Jan. 1, 1994.
- [5] J. Lilija and *et al.*, "Esterification of different acids over heterogeneous and homogeneous catalysts and correlation with the Taft equation," *Journal of Molecular Catalysis A: Chemical*, vol. 182-183, May. 31, 2002.
- [6] S. Dharne and V. Bokade, "Esterification of levulinic acid to n-butyl levulinate over heteropolyacid supported on acid-treated clay," *Journal of Natural Gas Chemistry*, vol. 20, Jan., 2011.
- [7] S. Sankar, V. Babu, R. Chada, D. Raju, and S. Rama, "Clean synthesis of alkyl levulinates from levulinic acid over one pot synthesized WO<sub>3</sub>-SBA-16 catalyst," *Journal of Molecular Catalysis A: Chemical*, vol. 426, Jan., 2017.
- [8] L. Negahdar, M. Al-Shaal, F. Holzhäuser, and R. Palkovits, "Kinetic analysis of the catalytic hydrogenation of alkyl levulinates to  $\gamma$ -valerolactone," *Chemical Engineering Science*, vol. 158, Feb. 2, 2017.
- [9] M. Silva, A. Lemos, F. Lima, A. Mendes, and M. Hernandez, "Heterogeneous Catalysts Based on H<sub>3</sub>PW<sub>12</sub>O<sub>40</sub> Heteropolyacid for Free Fatty Acids Esterification," *Intech Open*, Nov. 9, 2011.
- [10] M. Mesa and *et al.*, "Degradación fotocatalítica de Fenol, Catécol e Hidroquinona sobre nanomateriales Au-ZnO," *Revista Facultad de Ingeniería Universidad de Antioquia*, vol. 94, 2020.
- [11] P. Verma, K. Kaur, R. Kumar, and A. PalToor, "Esterification of acetic acid to methyl acetate using activated TiO<sub>2</sub> under UV light irradiation at ambient temperature," *Journal of Photochemistry and Photobiology A: Chemistry*, vol. 336, Mar. 1, 2017.
- [12] M. Cardoso, A. Posteral, A. Kopp, and C. Pérez, "Application of hydrothermally produced TiO<sub>2</sub> nanotubes in photocatalytic esterification of oleic acid," *Materials Science and Engineering: B*, vol. 206, Apr., 2016.
- [13] G. Corro, U. Pal, and N. Telleza, "Biodiesel production from Jatropa curcas crude oil using ZnO/SiO<sub>2</sub> photocatalyst for free fatty acids esterification," *Applied Catalysis B: Environmental*, vol. 129, Jan. 17, 2013.
- [14] J. Wen and *et al.*, "Photocatalysis fundamentals and surface modification of TiO<sub>2</sub> nanomaterials," *Chinese Journal of Catalysis*, vol. 36, Dec., 2015.
- [15] J. Murcia and *et al.*, "Methylene blue degradation over M-TiO<sub>2</sub> photocatalysts (M= Au or Pt)," *Ciencia en Desarrollo*, vol. 8, Jan., 2017.
- [16] L. Körösi and *et al.*, "Structural properties and photocatalytic behaviour of phosphate-modified nanocrystalline titania films," *Applied Catalysis B: Environmental*, vol. 77, Nov. 30, 2007.
- [17] K. Yang, Y. Dai, B. Huang, and M. Whangbo, "Density Functional Characterization of the Band Edges, the Band Gap States, and the Preferred Doping Sites of Halogen-Doped TiO<sub>2</sub>," *Chemistry of Materials*, vol. 20, Sept. 26, 2008.
- [18] J. Yu, Yu, Ho, Jiang, and Zhang, "Effects of F- Doping on the Photocatalytic Activity and Microstructures of Nanocrystalline TiO<sub>2</sub> Powders," *Chemistry of Materials*, vol. 14, no. 9, 2002.
- [19] J. Yu, W. Wang, B. Cheng, and B. Su, "Enhancement of Photocatalytic Activity of Mesoporous TiO<sub>2</sub> Powders by Hydrothermal Surface Fluorination Treatment," *The Journal of Physical Chemistry C*, vol. 113, no. 16, 2009.
- [20] J. Murcia, M. Hidalgo, J. Navío, J. Araña, and J. Rodríguez, "Study of the phenol photocatalytic degradation over TiO<sub>2</sub> modified by sulfation, fluorination, and platinum nanoparticles photodeposition," *Applied Catalysis B: Environmental*, vol. 179, Dec., 2015.
- [21] V. Guzmán, Y. Ortega, J. Salinas, A. López, and V. Collins, "TiO<sub>2</sub> Films Synthesis over Polypropylene by Sol-Gel Assisted with Hydrothermal Treatment for the Photocatalytic Propane Degradation," *Green and Sustainable Chemistry*, vol. 4, no. 3, 2014.
- [22] K. Murugan, T. Rao, G. Narashima, A. Gandhi, and B. Murty, "Effect of dehydration rate on non-hydrolytic TiO<sub>2</sub> thin film processing: Structure, optical and photocatalytic performance studies," *Materials Chemistry and Physics*, vol. 129, Oct. 3, 2011.
- [23] L. Kiyomi, R. Monteiro, N. Sanches, L. Dias, and O. Sala, "TiO<sub>2</sub> with a high sulfate content—thermogravimetric analysis, determination of acid sites by infrared spectroscopy and catalytic activity," *Catalysis Today*, vol. 85, Sep. 30, 2003.
- [24] S. Li and *et al.*, "Protonated titanate nanotubes as a highly active catalyst for the synthesis of renewable diesel and jet fuel range alkanes," *Applied Catalysis B: Environmental*, vol. 170-171, Jul., 2015.
- [25] K. Nandiwale and V. Bokade, "Esterification of Renewable Levulinic Acid to n-Butyl Levulinate over Modified H<sub>2</sub>ZSM<sub>5</sub>," *Chem. Eng. Technol.*, vol. 38, Jan. 27, 2015.
- [26] M. Al-Shaal and *et al.*, "Catalytic upgrading of  $\alpha$ -angelica lactone to levulinic acid esters under mild conditions over heterogeneous catalysts," *Catal. Sci. Technol.*, vol. 5, Jul. 15, 2015.
- [27] J. Ru, C. Hsu, and M. Jain, "Efficient photolytic esterification of carboxylic acids with alcohols in perhalogenated methane," *Tetrahedron Letters*, vol. 45, Jun., 2004.
- [28]